CDF/ANAL/TOP/CDFR/6921
Version 2.0
April 27, 2004

Measurement of $t\bar{t}$ in the e-τ_{had} and μ-τ_{had} Dilepton Channels

Sarah Demers, Jon Insler, Kevin McFarland, Tony Vaiciulis
(with the Top Dilepton Working Group)

University of Rochester

Contents

List of Tables

List of Figures

1 Introduction

This analysis seeks to measure the rate of $t\bar{t}$ events in the $e\tau_{had}$ and $\mu\tau_{had}$ dilepton final states using 193.5$\pm$12 pb^{-1} of data taken in the period from March 23, 2002 - September 2003.

The "$e\tau_{had}$" channel refers to events in the following decay chain:

$$t\bar{t} \rightarrow WWbb \rightarrow e\tau_{had}\nu_e\nu_\tau bb.$$

The "$\mu\tau_{had}$" channel refers to events in the following decay chain:

$$t\bar{t} \rightarrow WWbb \rightarrow \mu\tau_{had}\nu_\mu\nu_\tau bb,$$

where in each case τ_{had} refers to a τ decay with one or more hadrons in the final state.

Identification requirements for electrons and muons are identical to the tight-tight top dilepton analysis in the ee, $e\mu$, $\mu\mu$ channels as documented in Reference [2]. Of course, the present analysis differs in the requirement to identify a final state τ hadronic decay as well as the extra final state ν_τ from the τ decay which will change the measured $\not\!\!E_{\rm T}$ and H_t for these events.

The measured rate for $t\bar{t}$ in this channel can be expressed as

$$\sigma_{t\bar{t}} = \frac{N-B}{\epsilon_{t\bar{t}}^{e/\mu,\tau} * \mathcal{L}}$$

where:

- N is the number of signal events,
- B is the number of background events,
- $\mathcal{L}$ is the integrated luminosity of our data sample,
- and $\epsilon_{t\bar{t}}^{e/\mu,\tau}$ is our acceptance, which includes BR(dilepton$_{e/\mu,\tau}$) and BR($\tau \rightarrow$hadrons).

This note summarizes the expected signal, backgrounds and the calculation of the acceptance.

2 Event Selection

We use the "Winter Conference" tight electron and tight muon datasets created for the top and electroweak groups by Evelyn Thomson for top analyses [3]. We use the following cuts to select events:

1. **One Central Tight Electron, Tight CMUP Muon, or Tight CMX Muon above 20GeV**

   - We use the Baseline Analysis Cuts [4] used by the Dilepton Working Group for Winter Conferences. The tight electron cuts are listed in Table 1 and the tight muon cuts are listed in Table 2.

2. **Tau Cuts** as shown in Table 3

3. $\not\!\!E_{\rm T} > $ **20 GeV**

   - We use $\not\!\!E_{\rm T}$ corrected for tight muons, event vertex, and adjust for jet corrections of all jets > 15 GeV with $|\eta| < 2.0$.

4. **On subset of events, Veto events with 65GeV** $< M_{e/\mu,\tau} <$**115GeV**

   - This cut targets our $\gamma^*/Z \rightarrow \tau\tau + jets$ background, which was the largest background for this analysis in Run 1 [5]. We do not make this cut on all of the events, but only on a class of events with topology similar to $Z \rightarrow \tau\tau + jets$ in order to reduce our acceptance as little as is possible. As is described in Ref. [6], the event $\not\!\!E_{\rm T}$ is apportioned to the two presumptive taus (the hadronic tau and lepton candidates) in the invariant mass calculation according to the ϕ of the taus and the $\not\!\!E_{\rm T}$. We require that the two presumptive taus not be back-to-back in order for us to get an unambiguous answer in this procedure of dividing the $\not\!\!E_{\rm T}$:

     $$\Delta\phi_{\tau_{e/\mu},\tau_h} < (\ \pi \text{ - } 0.5)$$

     We make the following angular requirement in addition to the non-back-to-back requirement in order to select events that are $Z \rightarrow \tau\tau$ -like (with the $\not\!\!E_{\rm T}$ between the two presumptive taus in ϕ):

     $$(\Delta\phi_{\tau_{e/\mu},\not\!\!E_{\rm T}} + \Delta\phi_{\tau_h,\not\!\!E_{\rm T}} \text{ - } \Delta\phi_{\tau_{e/\mu},\tau_h}) < 0.4$$

where

- $\Delta\phi_{\tau_{e/\mu},\not\!\!E_{\rm T}}$ is the Phi between the electron or muon candidate and the event $\not\!\!E_{\rm T}$
- $\Delta\phi_{\tau_h,\not\!\!E_{\rm T}}$ is the Phi between the tau candidate (hadronically decaying tau) and the event $\not\!\!E_{\rm T}$
- $\Delta\phi_{\tau_{e/\mu},\tau_h}$ is the Phi between the electron or muon candidate and the hadronically decaying tau candidate

- Our Mass window is very wide (65–115GeV) because the resolution for this pseudo-invariant mass reconstruction is poor and because the mean value we reconstruct is systematically below the Z pole. If an event passes our angular requirements and is reconstructed in our mass window, we veto the event. This Z mass veto allows us to reduce our $\gamma^*/Z \rightarrow \tau\tau$ background by a factor of five while only reducing our acceptance by 4% [6].

5. **$H_t > 205$GeV**

   - Calculation of H_t uses corrected $\not\!\!E_{\rm T}$ and jet energies.
   - Our cut on the E_t of the first jet and on the event H_t were determined by an optimization procedure described in Ref. [7].

6. **$\geq$ 2 jets with $|\eta| < 2$**

   - E_T of first jet > 25GeV
   - E_T of second jet > 15GeV
   - We apply level5 jet energy corrections to all jets.

7. **opposite charge of tau and electron or muon**

   - the tau charge is the sum of charges of tracks within the tau cone around the tau seed track. As part of the tau selection, this total charge is required to be ± 1 for tau candidates with more than one track.

Variable	Cut
E_T	$>$ 20 GeV
P_T	$>$ 10 GeV
ISO4	$<$ 0.1
E_{had}/E_{em}	$<$ 0.055 + 0.00045*E
E/P	$<$ 2.0 (or $E_T >$ 50 GeV)
Lshr	$<$ 0.2
Q * Δx	-3.0 cm, 1.5 cm
$\mid \Delta z \mid$	$<$ 3.0 cm
χ^2_{strip}	$<$ 10
$\mid z^0 \mid$	$<$ 60.0 cm
track quality	$\geq$ 3 stereo SL $\geq$ 7 hits
	$\geq$ 3 axial SL $\geq$ 7 hits
FIDELE	1

Table 1: Electron identification cuts. Explanations of the variables are documented in Ref. [8].

Variable	Cut
Track P_T	$>$ 20 GeV
ISO4	$<$ 0.1
E_{had}	$<$ 6.0 GeV (and sliding for P above 100 GeV)
E_{em}	$<$ 2.0 GeV (and sliding for P above 100 GeV)
$\mid z^0 \mid$	$<$ 60.0 cm
$\mid D0 \mid$	$<$ 0.02 cm (with silicon)
	$<$ 0.2 cm (no silicon)
track quality	$\geq$ 3 stereo SL $\geq$ 7 hits
	$\geq$ 3 axial SL $\geq$ 7 hits
muon stub	has CMU and CMP stubs (for CMUP)
	has CMX stub (for CMX)
$\mid \Delta X_{CMU} \mid$	$<$ 3.0 cm (for CMUP muon)
$\mid \Delta X_{CMP} \mid$	$<$ 5.0 cm (for CMUP muon)
$\mid \Delta X_{CMX} \mid$	$<$ 6.0 cm (for CMX muon)

Table 2: Standard tight CMUP and CMX identification cuts.

Tau Variable	Cut
π^0 + Track P_T	$>$ 15 GeV
$\mid z_0 \mid$	$<$ 60 cm
$\mid D0 \mid$	$<$ 1 cm
(Track + π^0) Mass	$<$ 1.8 GeV/c^2
Cal Iso: ΔR=0.4/$E_T^{cluster}$	$<$ 0.06
# tracks in Iso Annulus	0
# π^0's in Iso Annulus	0
# tracks in Tau Cone	$<$ 4
$\mid \Sigma$(track charge) in Tau Cone$\mid$	1
μ veto: E_T/seed track P_T	$>$ 0.5
e veto: E_{HAD}/SUM (P)	$>$ 0.15
seed track quality	$\geq$ 3 stereo SL $\geq$ 7 hits $\geq$ 3 axial SL $\geq$ 7 hits
seed track $\mid$Z CES$\mid$	$>$ 9 cm $<$ 216 cm

Table 3: Tau identification cuts. Note that the tau cone and isolation annulus depend on the energy of the tau candidate.

3 τ ID Scale Factor

We take our tau ID efficiency from the Monte Carlo both to determine our acceptance to determine our backgrounds due to real taus ($Z \rightarrow \tau\tau$, WW, WZ.) In order to account for possible poor modeling of tau ID variables in the Monte Carlo we measure a tau ID scale factor using taus in the data. We then apply this scale factor to Monte Carlo in order to correctly reproduce the efficiency we see in the data. This exercise requires a clean sample of taus.

Our data comes from dataset ETAU08 where we have further required that the event passed the TAU_MET trigger path. This data sample, triggered on high missing Et and an isolated tau candidate, includes taus from W decays. We use the pythia $W \rightarrow \tau\nu$ Monte Carlo sample wtop1t to predict how many taus we expect to measure in the data. The difference between the number of taus we predict from the Monte Carlo and the number we observe in the data gives us a measure of the scale factor associated with our tau ID cuts. However, in order to compare the Monte Carlo with the data we need to correct for trigger efficiencies and backgrounds.

The TAU_MET path requires

- Level1: $\not\!\!E_{\rm T} > 25$ GeV
- Level3: $\not\!\!E_{\rm T} > 20$ GeV, ≥ 1 τ candidate

The Level3 τ candidate, found with TauFinderModule, has the following cuts:

- $E_t > 20$ GeV
- $|\text{detector } \eta| < 1$
- seed track $P_t > 4.5$ GeV
- seed tower $E_t > 6$ GeV
- no tracks in the 10-30 degree annulus around the seed track

We run TauFinderModule in the same standard configuration as is used in the trigger to reconstruct τ candidates. The 10-30 degree isolation annulus is not a part of identifying standard tau candidates with TauFinderModule so we add this isolation requirement to our Monte Carlo event selection.

We apply the following selection cuts to both data and Monte Carlo samples to isolate $W \rightarrow \tau\nu$:

- Passed TAU_MET path (data only.)
- No tracks in 10 to 30 degree isolation annulus (there is trememdous overlap between this cut and our isolation annulus tau ID cut.)
- Corrected $\not\!\!E_{\rm T} > 30$ GeV
- Tau candidate passes all ID cuts, with Track + π^0 P$_t$ > 25 GeV
- Veto events with $\geq$ one 5 GeV jet, $|\eta| < 2.0$ (dramatically reduces backgrounds.)

This sample is similar to the monojet sample studied in Ref. [9].

3.1 Corrections to Monte Carlo

We correct our Monte Carlo for the trigger efficiency of the Level1 $\not\!\!E_{\rm T}$ trigger using the turn-on curves shown in Ref. [9]. Our high $\not\!\!E_{\rm T}$ cut ensures that we never need to correct by a large factor because of the high trigger efficiencies at high $\not\!\!E_{\rm T}$.

We use the process $Z \rightarrow \mu\mu$ to understand the monte carlo modeling of our jet veto requirement. We isolate a clean sample of $Z \rightarrow \mu\mu$ in both the data's inclusive muon sample (193.5 pb^{-1}) and the Monte Carlo pythia ztop0m sample. We make the following cuts:

- Tight CMX or CMUP muon with P$t > 20$ GeV
- Track with P$t > 20$ GeV
- Muon and muon object (track) are back-to-back ($\Delta\phi > \pi - 0.5$)
- Reconstructed mass of the two objects is between 75 GeV and 105 GeV

We estimate our background in the data using the same-sign events as in Ref [10]. After background subtraction we have 72023 Monte Carlo events and 7091 data events. We plot the number of 5 GeV jets in the data and Monte Carlo in Figure 1 with both distributions normalized to unity. We see that 47% of the Monte Carlo events are in the 0 jet bin, which corresponds to our monojet sample, and 42% of the data falls in the 0 jet bin. This means that we need to scale our monte carlo monojet sample by a factor of 0.42/0.47 before we compare distributions

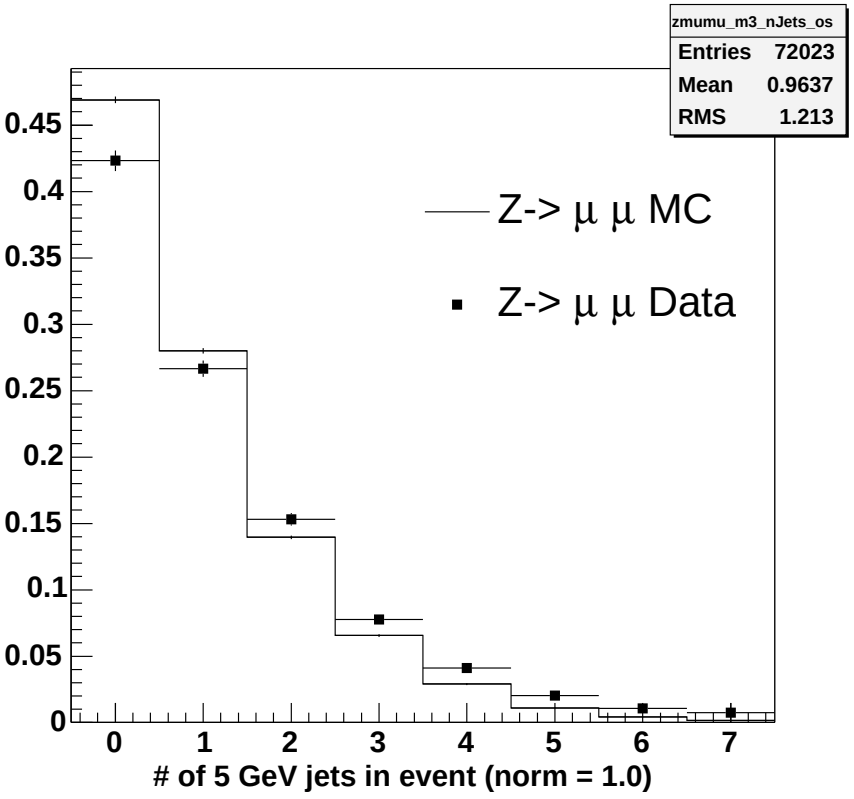

Figure 1: The distribution of the number of 5 GeV jets in $Z \rightarrow \mu\mu$ events in data and Monte Carlo. Both distributions have been normalized to unity.

with the data monojet sample. All plots of the $W \rightarrow \tau\nu$ Monte Carlo in this note have this monojet scale factor applied to them.

We must also scale for the luminosity of the samples involved. We use 57.6$\pm$3.4 pb^{-1} of Run2 data from the ETAU08 dataset. Assming a $W \rightarrow \tau\nu$ Cross Section * Branching Ratio of 2690$\pm$100 pb for wtop1t, we have the equivalence of 171$\pm$6 pb^{-1} of Monte Carlo [12]. In addition to the correction for the monojet cut we apply the correction for luminosity (57.6/171) to the Monte Carlo sample before we compare the Monte Carlo with the data.

3.2 Backgrounds

To convince ourselves that we do not need to worry about the QCD background we loosen our tau ID cuts so that we are only applying the following cuts:

- track + π^0 $P_t > 25.0$ GeV
- electron veto: HadE/ΣP > 0.15
- |charge of tau| = 1
- $>$ 4 tracks in tau cone

This is our sample of possible jet fakes to which we apply a modified relative fake rate calculated in Ref. [13] which we adjust to include the 10-30 degree track isolation annulus requirement in the denominator. This sample with the reduced tau ID cuts includes all of our final taus passing all cuts. This method is analogous to our method to determine our background due to jets faking taus in the main analysis, as described in section 5.1.1.

We apply this procedure to both the data, where we could presumably have some jet background, and to the Monte Carlo, where there is no jet background. We predict 53.7$\pm$ 14.0 events with the Monte Carlo and 56.8$\pm$14.8 events with the data where the errors given are due to the 26% systematic uncertainty associated with the jet to tau fake rate calculated in note 6784. Because these two numbers are consistent with each other we do not subtract any background from the monojet data sample due to jets faking taus.

The comparison can be seen between the Monte Carlo and data predictions in Figure 2, where we have dropped the cut on the tau charge and the cut on the number of tracks in the tau to show the track multiplicity distribution of the two

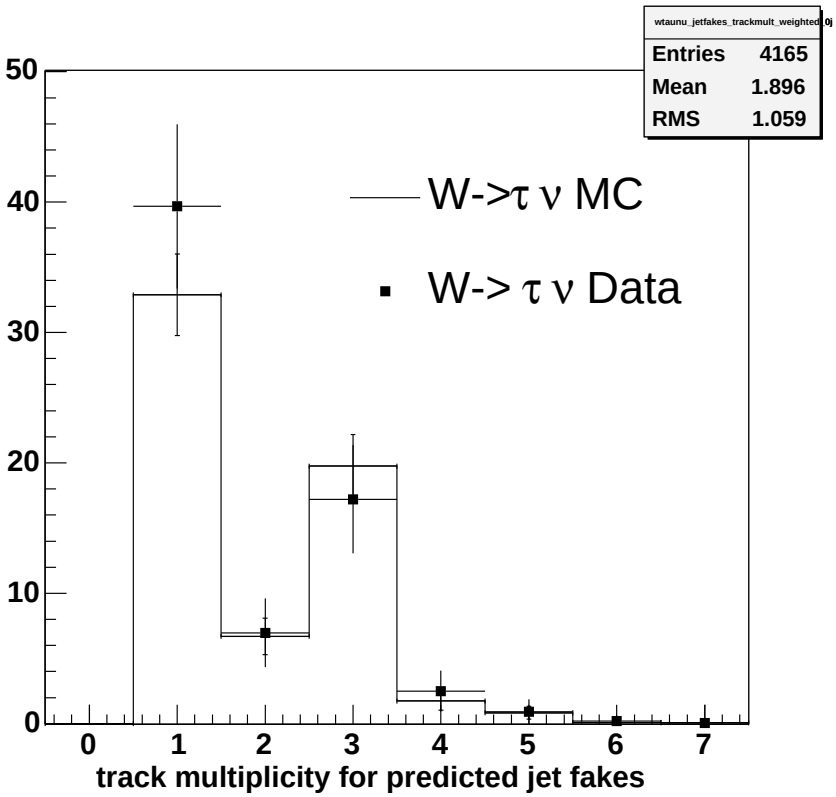

Figure 2: We show the predicted background from jet fakes in data and monte carlo. The agreement between the two where, in the Monte Carlo case we expect no background, gives us confidence to neglect this background.

samples. We see that the data is consistent with the distribution of pure taus in the Monte Carlo.

We reach a different conclusion with our electron background where we believe we are able to see a contribution coming from $W \rightarrow e\nu$. We create an electron sample by requiring the tau candidate to pass all tau ID cuts but fail the electron veto cut. We apply our calculated electron to tau fake rate to this sample (calculated in Ref. [20]) of (1.2$\pm$0.3)$\%$ which gives us a background contribution of 105.8$\pm$26.5 events due to electrons faking taus.

3.3 Scale Factor

We predict 583 events with the Monte Carlo and see 556 events in the data after subtracting the electron background. This gives us a scale factor of 0.95 $\pm$ 0.10 that we apply to the Monte Carlo. The largest contributions to the uncertainty, in decreasing order, are the uncertainty on the 57.6 pb^{-1} luminosity, the 2690 $\pm$ 100 pb cross section, and the 25% uncertainty on the electron background subtraction.

We show the track multiplicity distribution of our $W \rightarrow \tau\nu$ events, where we have removed the charge and number of tracks in tau cone cuts to see the shapes in Figure 3. We show the Monte Carlo stacked on top of the electron background contribution, allowing the total to be compared to the data points. Other comparisons, plotted in the same style but after all tau ID cuts, are shown in Figures 4 - 7. Note that the calorimeter isolation variable is not well modeled in the Monte Carlo (Figure 4.) We believe this discrepancy accounts for the majority of the measured scale factor.

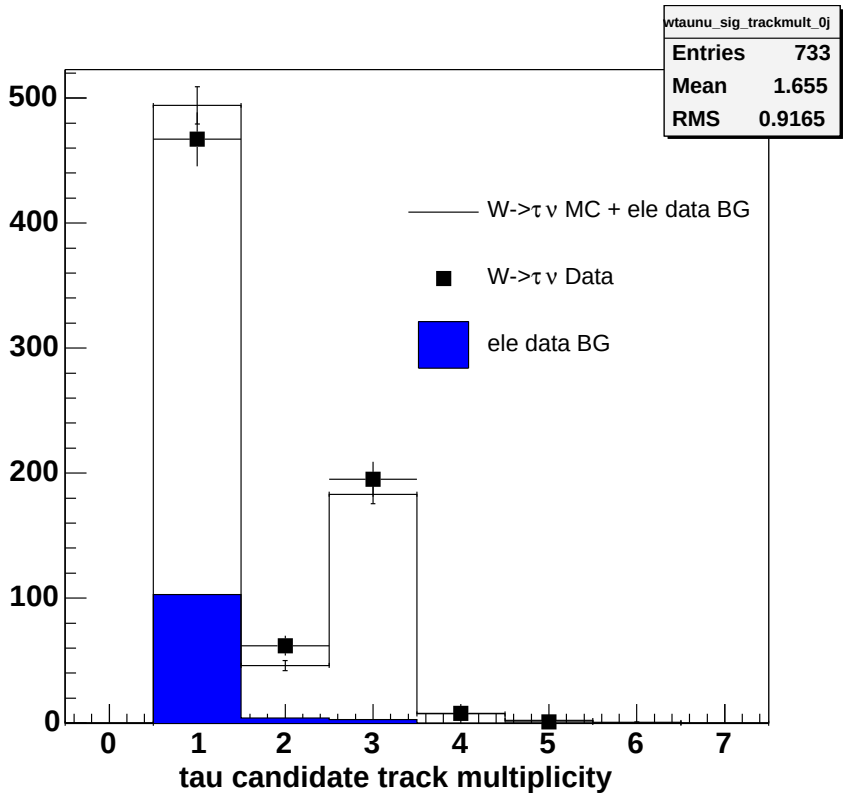

Figure 3: Final track multiplicity prediction in the data and the monte carlo. We show absolute predicted number of events from the Monte Carlo and measured events in the data before the electron subtraction. The electron background and Monte Carlo contributions have been stacked on top of each other so that the total can be compared to the data.

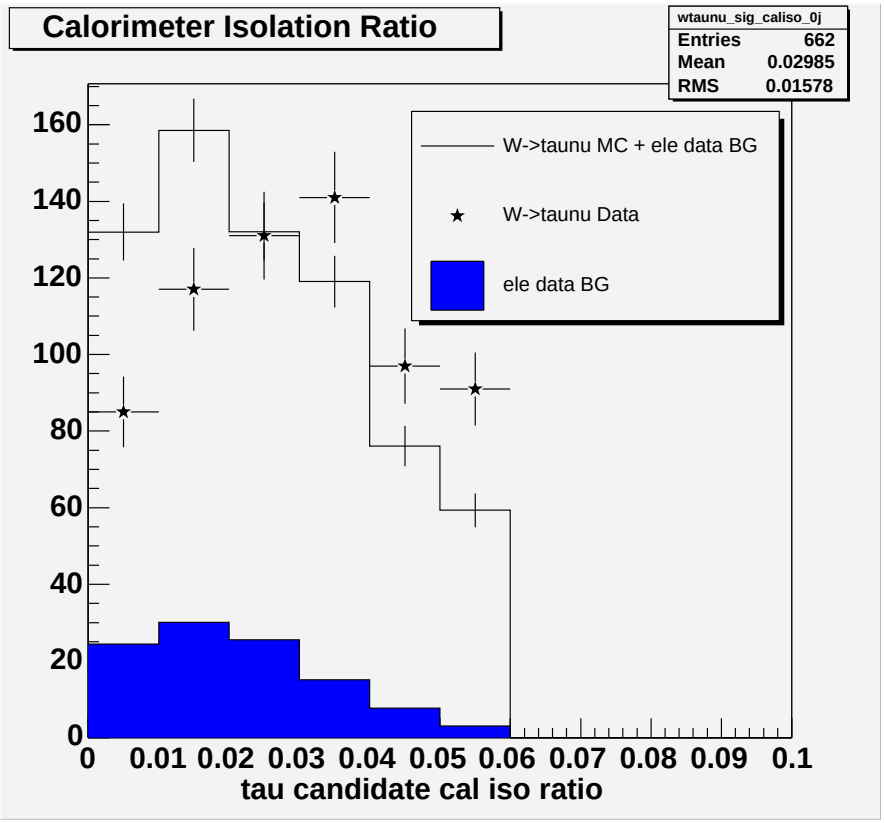

Figure 4: The data (points) and Monte Carlo plus electron background (histogram) calorimeter isolation ratio distributions are shown. Calorimeter isolation ratio is poorly modeled in the Monte Carlo which contributes to the overall scale factor that we must apply to our acceptance and to our real tau Monte Carlo backgrounds.

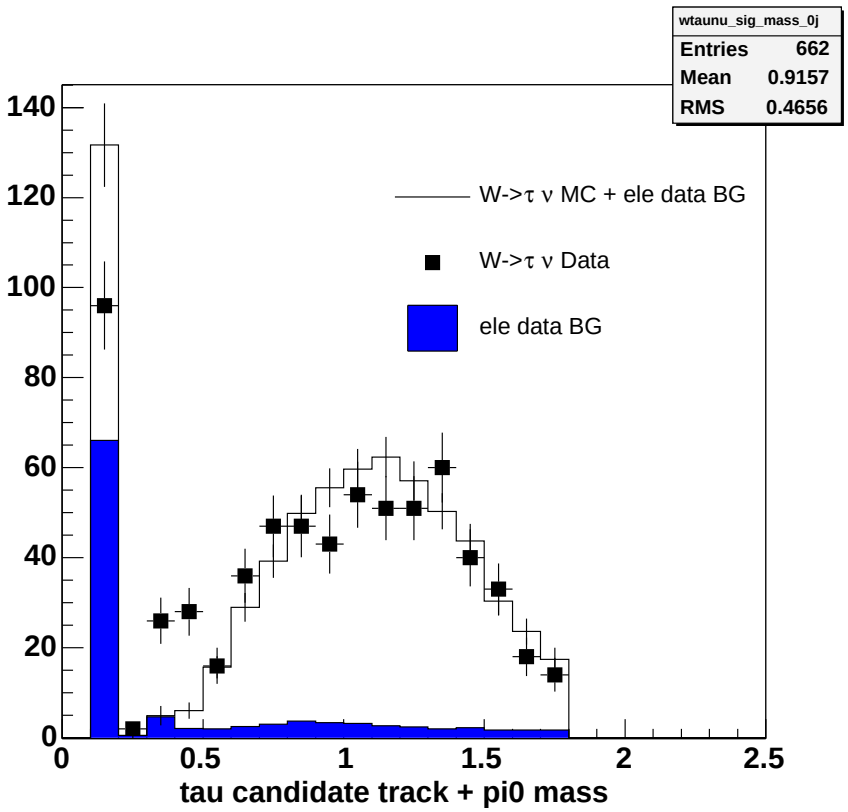

Figure 5: The data (points) and Monte Carlo plus electron background (histogram) tau candidate track + π^0 mass distributions are shown.

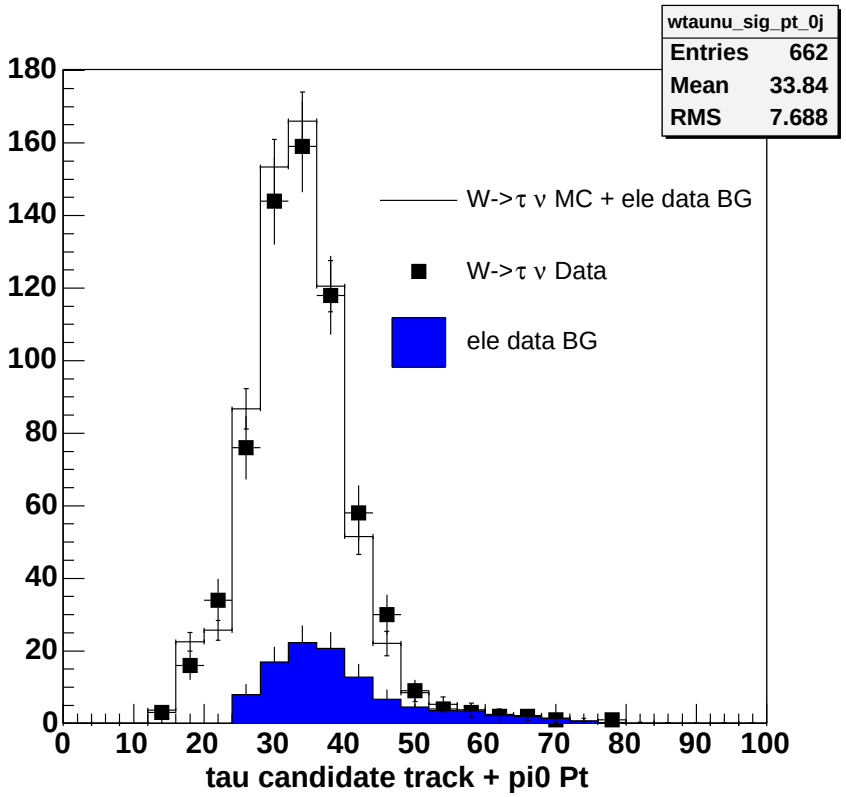

Figure 6: The data (points) and Monte Carlo plus electron background (histogram) track + π^0 P_t distributions are shown.

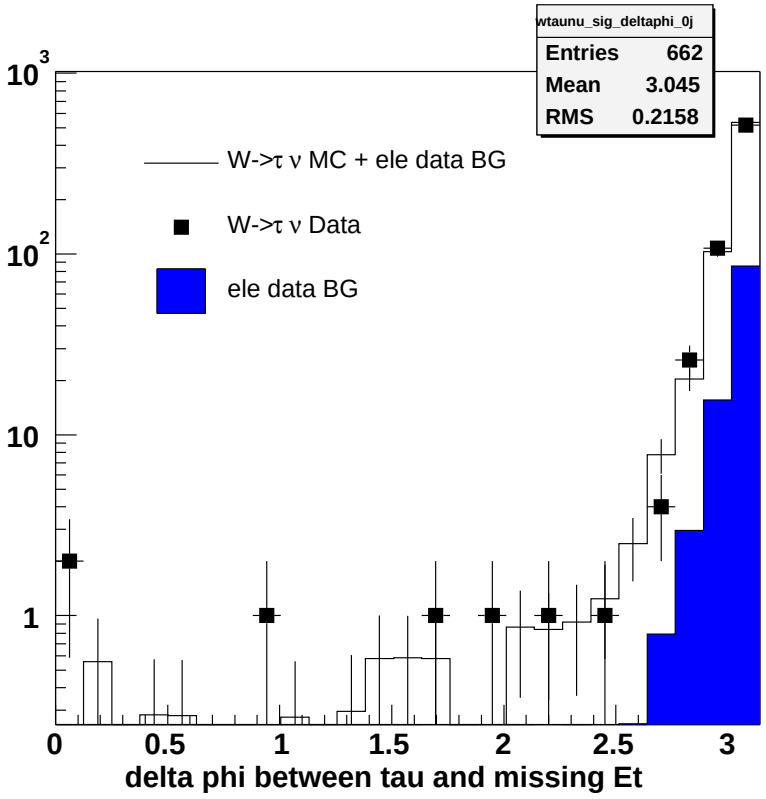

Figure 7: The data (points) and Monte Carlo plus electron background (histogram) $\delta\phi$ between the tau and the event $\not\!\!E_{\rm T}$ distributions are shown. We expect to see a peak at π for $W \rightarrow \tau\nu$ events.

4 Acceptance

We use the inclusive $t\bar{t}$ dataset ttopei as our primary Monte Carlo sample. This sample was generated with Pythia and simulated and reconstructed with release 4.11.1 of the CDF software. We processed the output of production with TopEventModule in order to recluster jets and correct $\not\!\!E_{\rm T}$ for the primary vertex and tight muons. We apply level5 jet corrections to the raw jets and we correct $\not\!\!E_{\rm T}$ and H_T to reflect the jet energy changes.

We do not do any matching of reconstructed objects to HEPG (generator-level) objects when we calculate our acceptance, but we do select our events using generator level information. One W must decay to a tau which must decay hadronically. The other W must decay to an electron or muon for the $e\tau$ and $\mu\tau$ channels respectively.

Our acceptance, $\epsilon_{t\bar{t}_{e/\mu,\tau}}$, can be written as:

$$\epsilon_{t\bar{t}_{e/\mu,\tau}} = \epsilon_{trigger}\ \epsilon_{geom-pt}\ \epsilon^{e/\mu}_{ID}\ \epsilon^{e/\mu}_{reco}\ \epsilon^{\tau}_{ID}\ \epsilon_{vertex}\ \epsilon_{\not\!\!E_{\rm T}}\ \epsilon_{H_T}\ \epsilon_{2jet}\ \epsilon_{OS}\ \epsilon_{Zveto}$$

We take the following pieces of the efficiency from the Monte Carlo:

- $\epsilon_{geom-pt}$, ϵ^{e}_{reco}, $\epsilon_{\not\!\!E_{\rm T}}$, ϵ_{H_T}, ϵ_{2jet}, ϵ_{OS}, ϵ_{Zveto}

The other pieces are shown in Table 4 [14][15][16][17][18].

We take the $p\bar{p} \rightarrow t\bar{t}$ cross section to be 6.7 pb from the NNLO calculations [19] when calculating our expected number of events.

4.1 Acceptance from ttbar MC

The effect of our analysis cuts is shown in Table 5. The cuts are defined as follows:

- N(sig): This is the true total number of events in the listed category according to HEPG information. The $e\tau$ category requires one of the W's to decay to an electron (and neutrino) and the other to decay to a tau. The $\mu\tau$ category requires one of the W's to decay to a muon and the other to decay to a tau. The $\tau\tau$ categories require both of the W's to decay to a tau with one tau decaying to a lepton and the other tau decaying hadronically.

- N($e\mu$ geoP$_{\rm T}$): requires a 20 GeV central, fiducial electron or muon.

	scale factor
$\epsilon_{trigger}$: CEM	0.966±0.001
$\epsilon_{trigger}$: CMUP	0.890±0.009
$\epsilon_{trigger}$: CMX	0.966±0.007
ϵ^{e}_{ID}: CEM	0.965±0.006
ϵ^{μ}_{ID}: CMUP	0.94±0.01
ϵ^{μ}_{ID}: CMX	1.015±0.007
ϵ^{μ}_{reco}: CMUP	0.927±0.010
ϵ^{μ}_{reco}: CMX	0.992±0.11
ϵ^{τ}_{ID}	0.95±0.10
ϵ_{vertex}	0.948±0.003

Table 4: Scale factors that must be applied to monte carlo acceptance (and Monte Carlo backgrounds.)

- N($e\mu$ id): requires the electron (CEM) or muon (CMUP or CMX) to pass the baseline winter conference ID cuts.

- N($e\mu$ iso): requires the electron or muon to pass the standard isolation cut.

- N(τ cand): requires a tau candidate (from TauFinderModule, with $|\eta| <$ 1.1) which does not match the reconstructed electron or muon. TauFinderModule requires a calorimeter tower with $E_T > 6$ GeV, no more than 5 shoulder calorimeter towers with $E_T > 1$ GeV and seed track $P_T > 4.5$ GeV. The decrease from 2034 to 1525 events is due mainly to events which are lost because the generated tau went into the forward region of the detector and therefore could not be found as a tau candidate which requires the object to be in the central calorimeter. Another contribution to the decrease is due to events in which the P_T of the generated tau is small enough that it can't be found as a tau candidate. The tau decay topology does not produce a particle which deposits 6 GeV E_T into a single calorimeter tower. Many of the events passing this cut only do so because a jet fakes a tau candidate in the central region while the generated tau goes into the forward region.

- N(τ P_T,id,iso): requires a tau candidate with $E_T > 15$ GeV to pass all tau ID and isolation cuts. There is a sharp decrease in number of events after this cut because many of the tau candidates correspond to jets which do not easily pass the tau ID cuts. The 15 GeV cut on tau E_T also contributes to

the decrease. The remainder of the decrease is due to the tau ID/isolation cuts.

- N(opp sign): requires the sum of the charged tracks in the tau cone to be opposite the charge of the e or μ (depending on the category).
- N(1jet): requires a minimum of one extra jet in the event that does not match the electron/muon or the tau (in a cone of radius 0.4) and has $|\eta| < 2.0$ and $E_T > 25$ GeV
- N(2jet): requires a second jet that does not match the electron/muon or tau and has $|\eta| < 2.0$ and $E_T > 15$ GeV.
- N($\not\!\!E_{\rm T}$): requires the corrected $\not\!\!E_{\rm T}$ (for tight muons and all jets with $\rm E_T > 15$ GeV and $|\eta| < 2.0$) to be above 20 GeV
- N($\rm H_T$): requires H_T to be above 205 GeV
- N(Z mass veto): requires the event to survive our mass reconstruction veto cut

Table 6 is a reordered version of the acceptance table which more clearly shows the separate effects of geometry, $\rm P_T$, ID and isolation cuts on the tau candidates. The N(τ geo$\rm P_T$) cut requires the reconstructed tau to match the generated tau. Here it is more clear that the combined efficiency of the tau ID and isolation cuts is about 35%. Note that both versions of the acceptance table have the same number of events passing all cuts, indicating that the normal analysis cuts accept events in the $t\bar{t}$ MC sample only if the reconstructed tau corresponds to the generated tau.

Our $t\bar{t}$ efficiency can be written as

$$\epsilon_{t\bar{t}}^{MC} = \text{(Total } N_{Zmass\ veto} \text{ / Total Sample Size) * scale factors,}$$

where the scale factors are weighted over the different efficiencies associated with the finding of the electron (CEM) or muon (CMUP or CMX) in the event. We therefore calculate

$$\epsilon_{t\bar{t}} = 0.00080 \pm 0.00005\text{(stat)} \pm 0.00014\text{ (sys)}$$

where the systematic errors are described in the following section.

	# of events			
Cut	eτ_h	$\mu\tau_h$	$\tau_e\tau_h$	$\tau_\mu\tau_h$
N(sig)	5545	5689	1000	1031
N($e\mu$ geoP$_{\mathrm{T}}$)	3373	2331	371	232
N($e\mu$ id)	2198	1983	178	195
N($e\mu$ iso)	2034	1828	156	172
N(τ cand)	1525	1419	117	134
N(τ P$_{\mathrm{T}}$,id,iso)	284	246	25	24
N(opp sign)	282	245	25	24
N(1jet)	274	240	22	24
N(2jet)	236	202	18	19
N($\not{E}_{\mathrm{T}}$)	219	185	18	18
N(H$_{\mathrm{T}}$)	200	171	17	15
N(Z mass veto)	193	164	16	14

Table 5: Number of events in Pythia signal Monte Carlo (dataset ttopei) passing each stage of the analysis cuts out of 386,037 events from this dataset.

	# of events			
Cut	eτ_h	$\mu\tau_h$	$\tau_e\tau_h$	$\tau_\mu\tau_h$
N(sig)	5545	5689	1000	1031
N($e\mu$ geoP$_{\mathrm{T}}$)	3373	2331	371	232
N(τ geoP$_{\mathrm{T}}$)	1323	957	160	84
N($e\mu$ id)	841	809	71	66
N(τ id)	469	463	39	40
N($e\mu$ iso)	440	425	35	34
N(τ iso)	284	246	25	24
N(opp sign)	282	245	25	24
N(1jet)	274	240	22	24
N(2jet)	236	202	18	19
N($\not{E}_{\mathrm{T}}$)	219	185	18	18
N(H$_{\mathrm{T}}$)	200	171	17	15
N(Z mass veto)	193	164	16	14

Table 6: Number of events in Pythia signal Monte Carlo dataset ttopei passing a reordered version of the analysis cuts. Here, the N(τ geoP$_{\mathrm{T}}$) cut requires the reconstructed tau candidate to match the generated tau.

Cut	Percentage of remaining τs
π^0 + Track $P_T > 15$ GeV	90.7%
$\mid z_0 \mid < 60$ cm	99.2%
$\mid D0 \mid < 1$ cm	100%
(Track + π^0) Mass < 1.8 GeV/c^2	95.6%
Cal Iso: ΔR=0.4/$E_T^{cluster} < 0.06$	77.9%
No tracks in Iso Annulus	84.1%
No π^0's in Iso Annulus	97.5%
# tracks in Tau Cone $< 4 = 1$	99.5%
$\mid \Sigma$(track charge) in Tau Cone $\mid$	92.0%
μ veto: E_T/seed track $P_T > 0.5$	99.7%
e veto: E_{HAD}/SUM (P) > 0.15	71.3%
seed track quality	98.8%
seed track $\mid$ Z CES $\mid$ (fiducial)	90.8%

Table 7: Effect of tau cuts on inclusive ttbar Pythia MC after a tight lepton (electron or muon) has been selected. An event must have a HEPG tau to make it to this point of the analysis but we have not required the tau to be a hadronically decaying tau. Electrons, unlike muons, are very efficiently reconstructed as taus because the energy they typically deposit in the calorimeter easily passes the threshold for tau reconstruction. Because of the efficient reconstruction of electrons as taus and because of the presence of electrons from tau decays, we are not surprised by the strength of the electron veto cut.

Category	Pythia	Herwig
$e\tau_h + \tau_e\tau_h$	0.76 ± 0.08	0.67 ± 0.06
$\mu\tau_h + \tau_\mu\tau_h$	0.53 ± 0.07	0.61 ± 0.06
total	1.29 ± 0.10	1.28 ± 0.08

Table 8: Number of expected events in 193.5 pb^{-1} for Pythia (ttop2e) and reweighted Herwig (ttopli) Monte Carlo samples.

Category	Pythia no ISR	Pythia default ISR
$e\tau_h + \tau_e\tau_h$	0.55 ± 0.06	0.62 ± 0.05
$\mu\tau_h + \tau_\mu\tau_h$	0.38 ± 0.06	0.46 ± 0.04
total	0.93 ± 0.08	1.08 ± 0.06

Table 9: Number of expected events in 193.5 pb^{-1} for Pythia ttop0e sample (no QED/QCD ISR) and Pythia ttopei sample (the default sample). The acceptance comparison is made before background subraction.

4.2 Systematics

- Jet Energy Corrections
  The level5 corrections to raw jet energies have some uncertainties associated with them which contribute to the systematic error. We estimate this systematic error using the standard procedure[1] in which we compare the acceptance when shifting all jet energies by $\pm 1\ \sigma$ of the combined uncertainty of the various jet corrections. Taking half the difference between the $+1\sigma$ and -1σ result yields a systematic uncertainty of 5.8%.

- MC generator Dependence
  We estimate the effect of a different modelling of $t\bar{t}$ production and decay by comparing the Pythia ttop2e dataset with Herwig dataset ttopli. Both are inclusive $t\bar{t}$ Monte Carlo samples. The ttop2e dataset has QED final state radiation (FSR) turned off to make a fair comparison with the Herwig sample which does not include QED FSR effects. We reweight the Herwig results by the factor $(0.108)^2/(0.111)^2$ to account for the fact that the Herwig sample uses the theoretical value of 0.111 for the $W \to l\nu$ branching ratio while Pythia uses the measured value of 0.108. The comparison is shown in terms of expected number of events in 193.5 pb^{-1} in Table 8. Because the two different datasets agree with each other within the statistical uncertainties, we quote a systematic uncertainty due to generator dependence equal to the 7% statistical uncertainty of the test.

- Initial State Radiation (ISR)
  We compare the acceptance determined from inclusive $t\bar{t}$ Pythia MC with ISR switched on (default dataset ttopei) and with ISR switched off (dataset ttop0e). Table 9 shows that the half difference of the ttop0e dataset with

[1] Documented at http://hep.physics.utoronto.ca/JeanFrancoisArguin/JetCorrDoc/SystUncert.html

Category	Pythia less FSR	Pythia more FSR
$e\tau_h + \tau_e\tau_h$	0.52 ± 0.04	0.52 ± 0.04
$\mu\tau_h + \tau_\mu\tau_h$	0.41 ± 0.04	0.37 ± 0.04
total	0.93 ± 0.06	0.89 ± 0.06

Table 10: Number of expected events in 193.5 pb^{-1} for Pythia ttopde sample (less FSR) and Pythia ttopee sample (more ISR).

respect to the default acceptance is 7%. This is taken as the systematic uncertainty.

- Final State Radiation (FSR)
  We estimate the acceptance uncertainty due to imprecise knowledge of Final State Radiation by comparing inclusive $t\bar{t}$ Pythia sample ttopde with less FSR (Kfactor is 2.0 for FSR evolution) with Pythia sample ttopee with more FSR (Kfactor is 0.5 for FSR evolution). Table 10 shows that the difference in acceptance is smaller than the statistical uncertainty of 7%, which we therefore use as an estimate of the systematic uncertainty.

- PDFs
  The default signal Monte Carlo sample, Pythia ttopei, is based on the CTEQ5L Parton Distribution Function set using $\alpha_s = 0.118$. We consider here the systematic uncertainty caused by varying the internal parameters of the PDF set as well as varying α_s and the choice of PDF group.

  With the new PDF set CTEQ6M, the CTEQ group made available 40 complementary PDF sets CTEQ6M.01...CTEQ6M.40 each of which represents an up or down variation along one of the twenty eigenvectors (corresponding to the $\sim$ 20 free parameters) which collectively form an orthonormal basis set spanning the PDF parameter space [1]. Each up and down variation pair represents the range of PDF behavior that is consistent with the current global data. Each event in the Pythia ttopei inclusive $t\bar{t}$ sample is reweighted according to the ratio of the CTEQ6M PDF values and the CTEQ6M.xx PDF values. [2] Then all normal selection cuts are applied using full simulation and reconstruction. The total acceptance change, with respect to CTEQ6M, caused by all of the variations is 0.6%.

[2] See April 2, 2004, Joint Physics Meeting minutes

In a similar way, a relative event by event reweighting is done using the CTEQ5L and MRST72 PDF sets resulting in a 0.8% change in acceptance due to the choice of PDF group. To estimate the acceptance sensitivity to the value of α_s we compare the PDF sets MRST72 ($\alpha_s = 0.1175$) and MRST75 ($\alpha_s = 0.1125$) using the reweighting procedure described above. The acceptance change is 0.1%. Considering the three contributions of 0.6%, 0.8%, and 0.1% we take 1% as the systematic uncertainty due to PDF uncertainty.

- Electron/Muon ID
  - The uncertainties in the reconstruction efficiencies ("scale factors") are summarized in Section 4 and are less than one percent. However, due to uncertainty in how the scale factor varies with the numbers of jets or the local environment, the $\{e + \mu\}$ dilepton anlaysis [2] chose a scale factor of 5%. [11] We follow this decision in our analysis.
- Tau ID
  - We measure this tau ID scale factor and calculate its systematic uncertainty by comparing $W \rightarrow \tau\nu$ data and Monte Carlo, as described in a previous section. We calculate a scale factor with an uncertainty of 10.5%.

We summarize the systematic uncertainty contributions in Table 11.

Source	Systematic Uncertainty
Jet Corr/Energy Scale	$\pm$5.8%
Electron/Muon ID	$\pm$5%
Tau ID	$\pm$ 10.5%
MC Generator	$\pm$7%
ISR	$\pm$7%
FSR	$\pm$7%
PDF	$\pm$1%
Total	17%

Table 11: Summary of Systematics for Acceptance

5 Backgrounds

5.1 Fakes

5.1.1 $j \to \tau$ Fakes

We have measured the rate at which a jet fakes a tau using the gqcd1g ("jet20"), gqcd2g ("jet50"), gqcd3g ("jet70"), and SUMET datasets [13]. The fake rate was calculated as a function of corrected jet E_t and calorimeter isolation where the denominator jets consisted of non-trigger-biased jets after requiring

- jet matches to tau candidate,
- $E_T > 15$GeV,
- electron veto ($E_{HAD}/\Sigma(P) > 0.15$),
- track charge in tau cone = ± 1,
- and number of tracks in tau cone < 4,

and where the numerator was the subset of these events that passed all tau ID cuts.

The fake rates measured in the different samples are marginally statistically inconsistent, and so we choose to calculate fake rates from the jet50 sample with a systematic uncertainty of 26% to cover these differences [13].

Note that this is a relative fake rate (requiring a tau candidate in the denominator) in order to allow us to remove electron veto events (see the e$\rightarrow \tau$ fake section) and to look at our jet fake contribution as a function of the charge product of the tau candidate and other lepton in our jet multiplicity studies of Section 6.

In order to determine our background due to fakes we select a sample of tau candidates from both the tight electron and tight muon datasets that pass the fake rate demoninator cuts as well as the following event selection cuts:

- One central tight electron, CMUP muon or CMX muon above 20GeV as in Ref. [2]
- One central jet ($|\eta| < 1.1$) that matches to a tau candidate passing the denominator cuts shown above
- event corrected $\not\!\!E_{\rm T} > 20GeV$
- $\geq$ 2 jets with $|\eta| < 2$
  - E_T of first jet $>$ 25GeV
  - E_T of second jet $>$ 15GeV
- $H_T > 205$GeV
- opposite charge of tau candidate and electron/muon

Note that if an event has more than one tau candidate that passes the denominator fake rate cuts it may be entered into our denominator background sample more than once.

This fake rate sample, which we believe to be dominated by W+jet events, does contain both our signal and other sources of real taus ($Z \rightarrow \tau\tau$, WW, WZ) In order to account for this we apply the fake rate only to events where the tau candidate passes the above cuts but fails the final tau ID cuts. To avoid undercounting our fakes this way, we replace our measured relative fake rate, f, with the fake rate corrected for the missing fake taus, $f/(1-f)$. As the fake rate is of order 1% on average, this is practically of little consequence, but it does minimize double counting signal into the jet fakes.

We have 67 background candidate events in the e,τ channel and 37 background candidate events in the μ,τ channel to which we apply the fake rate. The total background in 193.5 pb^{-1} is 0.45$\pm$0.10$\pm$0.12 events for the e,τ channel and 0.30$\pm$0.06$\pm$0.08 events in the μ,τ channel. The contribution of the events to the background as a function of tau candidate track + π^0 Pt can be seen in Figure 8.

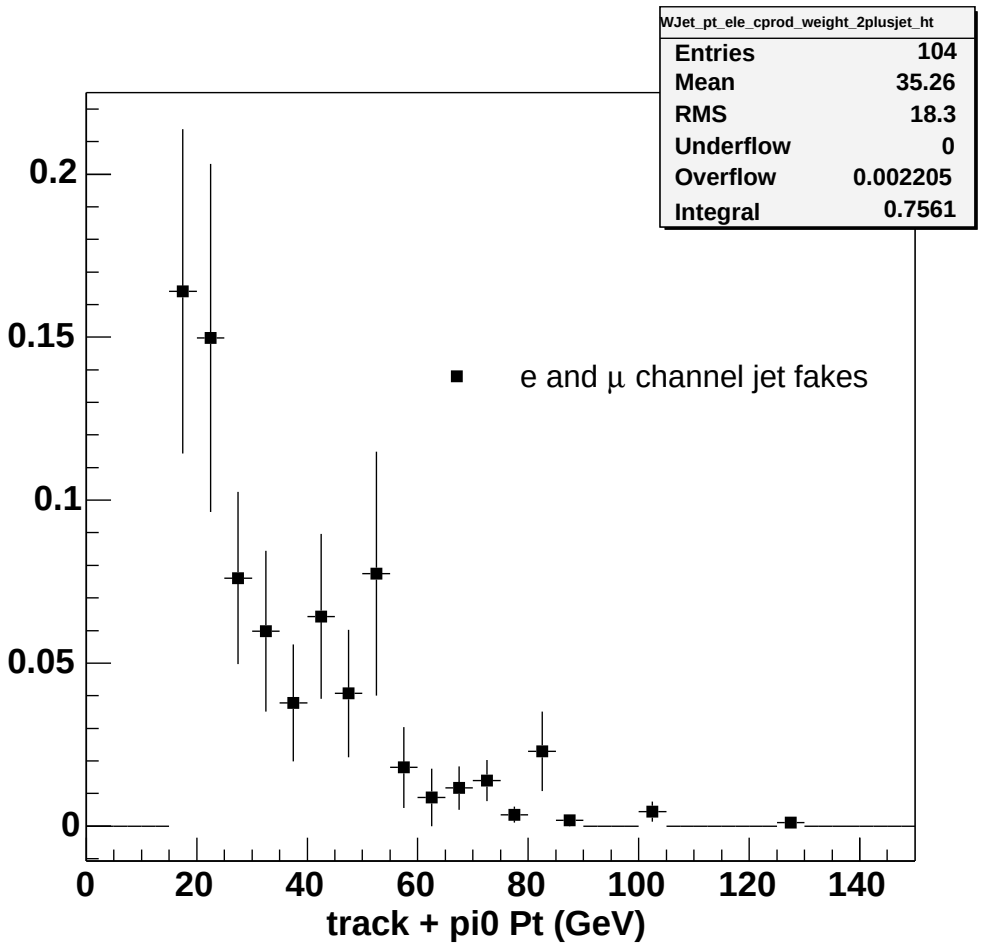

Figure 8: The background contribution due to jets faking taus is shown as a function of tau candidate track + π^0 P_t for the combined e, τ channel and μ, τ channel.

5.1.2 $e \rightarrow \tau$ Fakes

We measured the rate at which an electron fakes a tau using $Z \rightarrow ee$ events in the data [20]. The value of the fake rate was calculated as a function of our electron veto variable, $E_{HAD}/\Sigma(P)$. We use a cut value of $E_{HAD}/\Sigma(P)$ <0.15 to define our electron sample. The measured $e \rightarrow \tau$ fake rate at this value is (1.2±0.3)%.

We count the number of events in the data that pass all of our event selection cuts where the tau candidate passes all tau ID cuts except it fails our electron veto cut. There are 8 events before the H_t cut, and we plot the $E_{HAD}/\Sigma(P)$ of these events in Figure 9 to assure ourselves that they are electron-like. The peak at zero gives us evidence of this. After the H_t cut we have seven events that pass all cuts except for the electron veto. Applying our fake rate to this sample gives us a background of 0.08±0.03(stat)±0.02(sys) events. Note that this background includes the physics background of $Z \rightarrow ee$ events and is only a background in the e, τ channel.

5.1.3 $\mu \rightarrow \tau$ Fakes

A muon is unlikely to fake a tau because muons usually deposit very little energy into the calorimeter and a minimum of 6 GeV of calorimeter energy is required in order to form a tau candidate. The physics source for this background is $Z \rightarrow \mu\mu$ events.

We measured the rate of muons faking taus in the data using $Z \rightarrow \mu\mu$ events and found it to be consistent, within errors, to the fake rate given by the Monte Carlo [10]. We see from this study that our muon veto variable, E_T/ seed track P_T, is well modeled in the monte carlo. Since we have confidence in the Monte Carlo, and because it is difficult to isolate the few muons faking tau candidates in the data (and even if we could we would be plagued by low statistics and therefore high uncertainties) we calculate this background using $Z \rightarrow \mu\mu$ Monte Carlo.

To estimate the background for events with zero or one jet in the final state, we use 1000000 events from the pythia ztop0m monte carlo dataset. However there are not enough statistics in this dataset for us to determine the ≥2 jet bin contribution, after all cuts, to the total background. For this, we use 284946 events from the Herwig + ALPGEN (+ 2 parton) $Z \rightarrow \mu\mu$ Monte Carlo sample, atop27. The latter sample sample has a Cross Section * Branching ratio of approximately 23 pb. After all cuts, we predict a background contribution of 0.05±0.03 events for 193.5 pb^{-1}.

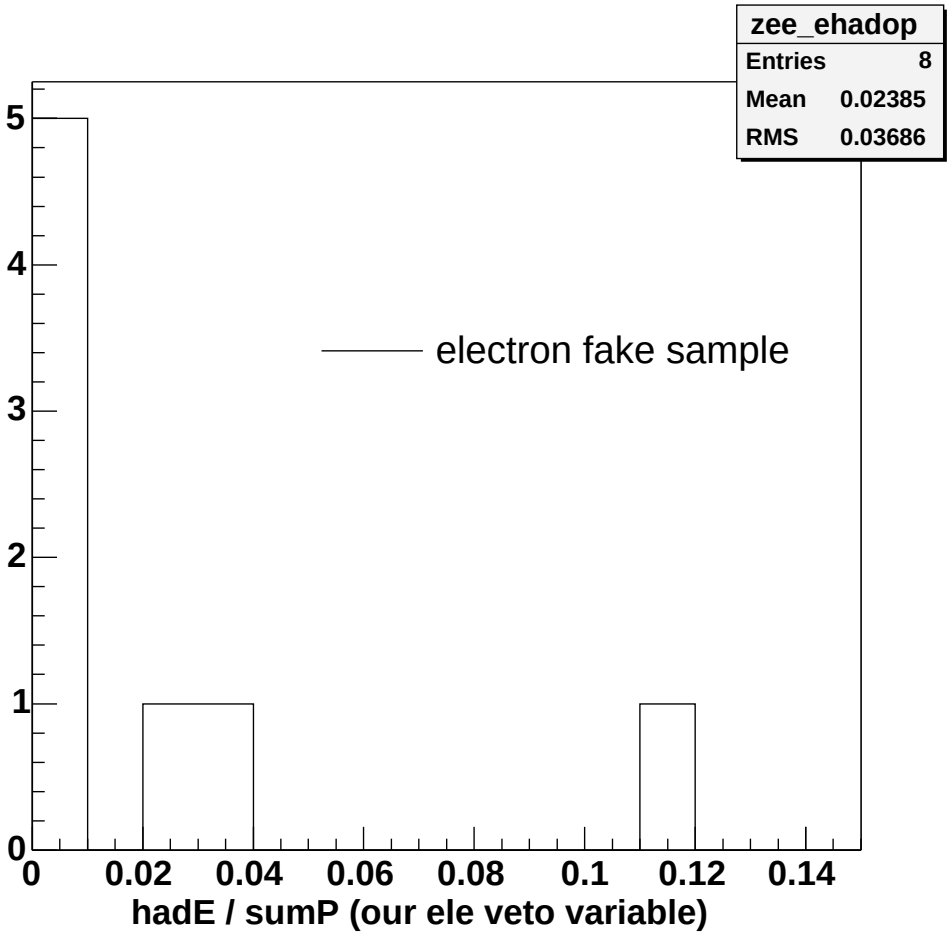

Figure 9: The electron veto variable, $E_{HAD}/\Sigma(P)$, for our electron candidate events before the H_t cut. The peak at zero gives us confidence that this sample is dominated by real electrons. Applying the H_t cut brings the sample to 8 events.

5.2 $\gamma^+/Z \rightarrow \tau\tau + jets$

We use 464433 events from the ztop1t $\gamma^*/Z \rightarrow \tau\tau$ Pythia Monte Carlo sample to determine the contribution from this background as a function of jets for the jet multiplicity tables. The cross section * branching ratio of this sample is 283.5 pb. unfortunately only one event from this sample passes all of our analysis cuts. Therefore, to estimate the background contribution after all cuts we use Herwig + APLGEN (+2 parton) Monte Carlo.

There are three datasets covering three mass regions that need to be taken into account for the Herwig + Alpgen (+2 parton) Monte Carlo:

- Dataset atop2b: We ran on a sample of 286823 events from this dataset. These events were generated in the Z mass window, with masses between 75GeV and 105GeV. The cross section * branching ratio is 23.3 $\pm$0.1pb.
- Dataset atop66: We ran on a sample of 274295 events from this dataset. These events have generated masses between 10GeV and 75GeV. The cross section * branching ratio is 50.2 $\pm$0.1 pb.
- Dataset atop63: We ran on a sample of 166942 events from this dataset. These events have generated masses between 105GeV and 800GeV. The cross section * branching ratio is 0.631 $\pm$ 0.001 pb.

The contribution due to each Monte Carlo sample is shown for both the e, τ channel and the μ, τ channel in Table 12, after all relevant Monte Carlo scale factors have been applied. The Pythia background based on the one event is listed for completeness but it is not used in the analysis. Note that our expected number of background events from $\gamma^+/Z \rightarrow \tau\tau$ is one fourth the size of our expected number of signal events. This is very different from this analysis in Run 1 where the background from this physics process was larger than the expected signal. The mass veto cut is responsible for the dramatic reduction of this background [6].

5.3 WW

We calculate our jet multiplicity contributions from WW with 195897 events from the Herwig + Alpgen (+0 parton) Monte Carlo sample atop4x. This sample has a cross section * branching ratio of 8.282$\pm$0.005 pb. We calculate our background contribution with 828061 WW events from the Herwig + Alpgen (+1 parton) sample atop5x. This sample has a cross section * branching ratio of 4.363$\pm$0.003pb.

We apply all relevant Monte Carlo scale factors. Our resulting background for the e, τ channel is 0.08$\pm$0.01 events and for the μ, τ channel we see a background of 0.06$\pm$0.01 events. These final background numbers are consistent with what we calculate if we sample atop4x to predict ourbackground.

5.4 WZ

We calculate our WZ background and jet multiplicity study contributions with 152500 events from the Herwig + Alpgen (+0 parton) monte carlo sample atop0y. This sample has a cross section * branching ratio of 2.367$\pm$0.001 pb. After all analysis cuts we have eight events in both the e, τ and μ, τ channels. Our resulting backgrounds, after all relevant Monte Carlo scale factors have been applied, are 0.01$\pm$0.01 events for both channels.

5.5 Background Summary

We show a summary of our backgrounds in Tables 13 and 14.

dataset	Generated Z Mass range	# of e, τ BG events	# of μ, τ BG events
atop2b	75-105GeV	0.09$\pm$0.04	0.06$\pm$0.03
atop66	10-75GeV	0.00+0.03	0.00+0.03
atop63	105-800GeV	0.06$\pm$0.01	0.05$\pm$0.01
Total Herwig+Alpgen	10-800GeV	0.15$\pm$0.05	0.11$\pm$0.04
Pythia ztop1t	$\geq$30GeV	0.11$\pm$0.11	0.10$\pm$0.10

Table 12: Summary of backgrounds from $\gamma^*/Z \rightarrow \tau\tau + jets$. The pythia prediction, which is not used, is listed for comparison.

	number of events expected
$\gamma^*/Z \to \tau\tau + jets$	0.15 $\pm$0.05(stat) $\pm$0.03(sys)
$j \to \tau$ fakes	0.45 $\pm$0.10(stat) $\pm$0.12(sys)
$e \to \tau$ fakes	0.08 $\pm$0.03(stat) $\pm$0.02(sys)
WW	0.08 $\pm$0.01(stat) $\pm$0.02(sys)
WZ	0.01 $\pm$0.01(stat)
Total expected background events	0.77 $\pm$0.12(stat) $\pm$ 0.13(sys)
Signal exp from MC	0.59 $\pm$0.05(stat) $\pm$0.10(sys)

Table 13: e, τ channel signal and background predictions

	number of events expected
$\gamma^*/Z \to \tau\tau + jets$	0.11 $\pm$0.04(stat) $\pm$0.02(sys)
$j \to \tau$ fakes	0.30 $\pm$0.06(stat) $\pm$0.08(sys)
$Z \to \mu\mu$	0.05 $\pm$0.03(stat)
WW	0.06 $\pm$0.01(stat) $\pm$0.01(sys)
WZ	0.01 $\pm$0.01(stat)
Total expected background events	0.53 $\pm$0.08(stat) $\pm$0.08(sys)
Signal exp from MC	0.44 $\pm$0.04(stat) $\pm$0.07(sys)

Table 14: μ, τ channel signal and background predictions

6 Jet Multiplicity Analysis

This analysis was performed blinded to possible events that passed the signal criteria in the data. As an *a priori* criterion for ensuring that we were ready to look at the data in the signal region, we studied agreement in related event samples that are not in our signal region because of lower jet multiplicity (zero or only one extra jet). In order to study this sample, it is also necessary to drop the H_T and Z mass removal cuts from the analysis because of their correlation with the jet multiplicity. To expand the same and test different background regions, we also considered the rate of same sign lepton events in the zero and one jet multiplicity bins.

As part of the blinding procedure, we did not look at the data[3] with jet multiplicity ≥ 2 for either opposite or same sign lepton pairs. The decision to look at these samples was only made after fixing the event selection and performing statistical checks for consistency with the background predictions.

The results of this jet multiplicity studies for the zero and one jet bins (with no H_T requirement are shown in Tables 15–18.

To check consistency with the predictions, a joint probability of these low jet multiplicity observations, given the predicted rates, was formed. In order to account for the uncertainties in the predicted rates, this probability was compared against the probabilities of pseudo experiments which chose "true" predictions from the measured predictions and their errors, and then generated Poisson fluctuations about those "true" means. The main *a priori* test that we chose was to look at all eight of the values for opposite and same sign, zero and one jet multiplicity, electron and muon data samples, and this resulted in a probability which was higher than in 40% of generated pseudo experiments. The distribution of these probabilities by percentile and the identified value in the data are shown in Figure 10.

We also performed a number of similar tests on subsets of the low jet multiplicity data in order to test for consistency with a variety of pathologies. Table 19 summarizes these tests and their results. The least probable agreement is in the zero jet, opposite sign muon case, where the probability is in the 5^{th} percentile.

[3] with one exception: there was an aborted attempt to prebless this result only in the $e\tau_{had}$ channel with the 72 pb$^{-}1$ dataset. Before that result reached the preblessing stage, but after the events were unblinded, the decision was reached not to take the analysis to a final result. At that time, there were no events observed in the signal region for this subset of the $e\tau$ sample.

sample	0 jets	1 jet	$\geq$2 jets
$jet \to \tau$ fakes	12.54±0.57±3.26	2.35±0.22±0.61	0.92±0.13 ±0.24
$e \to \tau$ fakes	0.92±0.10±0.23	0.22±0.05±0.05	0.10±0.03±0.03
$\gamma^*/Z \to \tau\tau$	8.15±1.07±0.86	1.79±0.50±0.19	0.89±0.18±0.09
WW	2.66±0.17±0.28	0.22±0.02±0.02	0.10±0.01±0.01
WZ	0.03±0.01	0.07±0.02	0.02±0.01
Signal ($t\bar{t}$)	0.03±0.01	0.12±0.02±0.01	0.70±0.05±0.07
Total Expected	24.3±1.2±3.4	4.8±0.6±0.6	2.7±0.2±0.3
Data	17	5	**blind**

Table 15: Jet multiplicity table for e-tau channel, opposite sign events.

sample	0 jets	1 jet	$\geq$2 jets
$jet \to \tau$ fakes	11.70±0.58±3.04	1.29±0.17±0.34	0.53±0.08±0.14
$\gamma^*/Z \to \mu\mu$	3.40±0.36	0.22±0.09	0.08±0.06
$\gamma^*/Z \to \tau\tau$	4.49±0.82±0.44	0.95±0.38±0.10	0.95±0.38±0.10
WW	2.03±0.15±0.21	0.19±0.02±0.02	0.10±0.01±0.01
WZ	0.05±0.01	0.03±0.01	0.02±0.01
Signal ($t\bar{t}$)	0.01±0.01	0.10±0.02±0.01	0.52±0.05±0.05
Total Expected	21.7±1.1±3.1	2.8±0.4±0.4	2.2±0.4±0.2
Data	11	4	**blind**

Table 16: Jet multiplicity table for mu-tau channel, opposite sign events.

sample	0 jets	1 jet	$\geq$2 jets
$jet \to \tau$ fakes	6.86±0.39±1.78	1.87±0.19±0.49	1.05±0.13±0.27
$e \to \tau$ fakes	0.02±0.01	$0^{+0.01}_{-0}$	$0^{+0.01}_{-0}$
$\gamma^*/Z \to \tau\tau$	0.30±0.20	0.0+0.11	0.02±0.02
WW	0.06±0.02	0.005±0.003	0.005±0.003
WZ	0.05±0.01	0.03±0.01	0.01±0.01
Signal ($t\bar{t}$)	$0^{+0.003}_{-0}$	0.003±0.003	$0^{+0.003}_{-0}$
Total Expected	7.3±0.4±1.8	1.9±0.2±0.6	1.1±0.1±0.3
Data	8	3	**blind**

Table 17: Jet multiplicity table for e-tau channel, same sign events.

sample	0 jets	1 jet	$\geq$2 jets
$jet \to \tau$ fakes	5.34± 0.36±1.39	0.78±0.15±0.20	0.51±0.14±0.13
$\gamma^*/Z \to \mu\mu$	0.08±0.08	$0^{+0.04}_{-0}$	0.10±0.04
$\gamma^*/Z \to \tau\tau$	0.10±0.10	0	0.01±0.01
WW	0.02±0.01	0.004±0.002	0.003±0.002
WZ	0.05±0.01	0.03±0.01	0.01±0.01
Signal ($t\bar{t}$)	0	0	0.002±0.002
Total Expected	5.6±0.4±1.4	0.8±0.2±0.2	0.6±0.2±0.1
Data	3	0	**blind**

Table 18: Jet multiplicity table for mu-tau channel, same sign events.

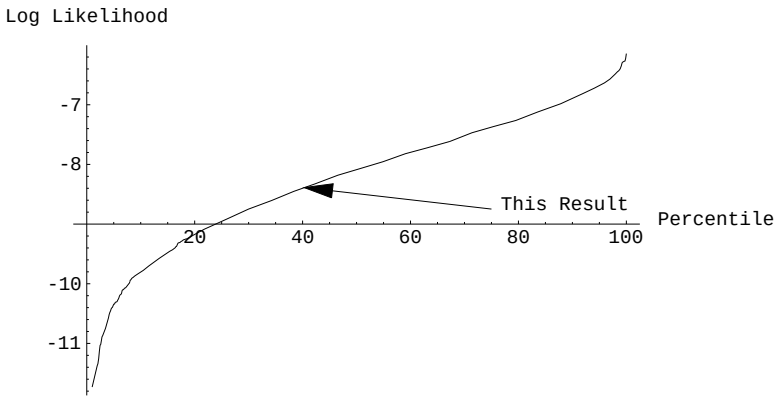

Figure 10: The *a priori* test of the data probability of the observed low jet multiplicities compared against the predictions shown with the distribution of the same quantity in pseudo experiments. The pseudo experiments have a lower probability 40% of the time.

Subsamples included	Probability Percentile
All electron bins	62
All muon bins	20
All opposite sign bins	16
All same sign bins	78
Electron and muon zero jet opposite sign	9
Only muon zero jet opposite sign	5

Table 19: Consistency tests applied to the low jet multiplicity data

6.1 The Unblinded Data Samples

Having passed the *a priori* criterion for agreement, we then examine the signal regions and same sign region. With no H_T or Z mass cut, the results are shown in Table 20. Electron same and opposite sign rates appear higher than predicted, whereas muon rates are consistent. However, upon applying the final event selection cuts, including the H_T and Z mass requirement, the results in Table 21 are obtained where no visible disagreement is evident. We show the Run1 predicted and measured events in Table 22. In total, we have two candidate signal events (both $e\tau$ events) and one same sign event which would otherwise pass signal criteria ($e\tau$). These events are:

- Run = 167299, Event = 2376337, Njets = 3, H_T = 286 GeV, MET = 59.4 GeV (opp sign eτ candidate). See Table 23 and Fiure 11. One jet is b-tagged.
- Run = 151434, Event = 158200, Njets = 2, H_T = 239 GeV, MET = 71.7 GeV (opp sign eτ candidate). See Table 24 and Figure 12. No jets are b-tagged.

The thirteen events in the $\geq$2 jet bins of the Njet tables were checked for b-tagged jets but none were found except in run 167299, event 2376337. This is consistent with the hypothesis that these bins are dominated by background processes that do not contain b quarks.

Sample	OS e	SS e	OS μ	SS μ
Background	2.03±0.2±0.3	1.1±0.1±0.3	1.7±0.4±0.2	0.6±0.2±0.2
$t\bar{t}$	0.70±0.05±0.07	<0.003	0.52±0.05±0.05	0.002±0.002
Data	8	4	1	0

Table 20: The ≥ 2 jet multiplicity data where the $t\bar{t}$ signal is expected compared to predictions. No H_T or Z mass cut has yet been applied.

Sample	OS e	OS μ
Background	0.77±0.12±0.13	0.53±0.0.08±0.08
$t\bar{t}$	0.59±0.05±0.10	0.47±0.04±0.07
Data	2	0

Table 21: The signal region, including the H_T, Z mass, opposite charge and ≥ 2 jet multiplicity requirements

Background	2.50±0.43
$t\bar{t}$	1.1±0.4
Data	4

Table 22: We show here the results of the Run1 tau dilepton analysis [22]. The expected number of events shown above was calculated with the Run1 CDF measured value of the $t\bar{t}$ cross section of $7.7^{+1.8}_{-1.5}$pb. In the Run2 analysis we document in this note we use the theoretical value of the cross section. The corresponding value for Run1 conditions is 4.8 $\pm$0.7pb [23].

Object	E_T (GeV)	Pseudorapidity	Phi (rad/deg)
electron	39.8	-0.28	1.1(61)
tau	38.6	-0.95	3.8(215)
jet	73.3	-0.27	2.9(166)
jet	39.5	-1.48	0.2(12)
jet	35.4	-1.40	0.8(45)

Table 23: Details for run 167299, event 2376337.

Object	E_T (GeV)	Pseudorapidity	Phi (rad/deg)
electron	78.9	-0.99	1.7(98)
tau	20.0	-0.60	3.8(218)
jet	34.9	-0.92	1.2(71)
jet	33.6	0.30	5.0(286)

Table 24: Details for run 151434, event 158200.

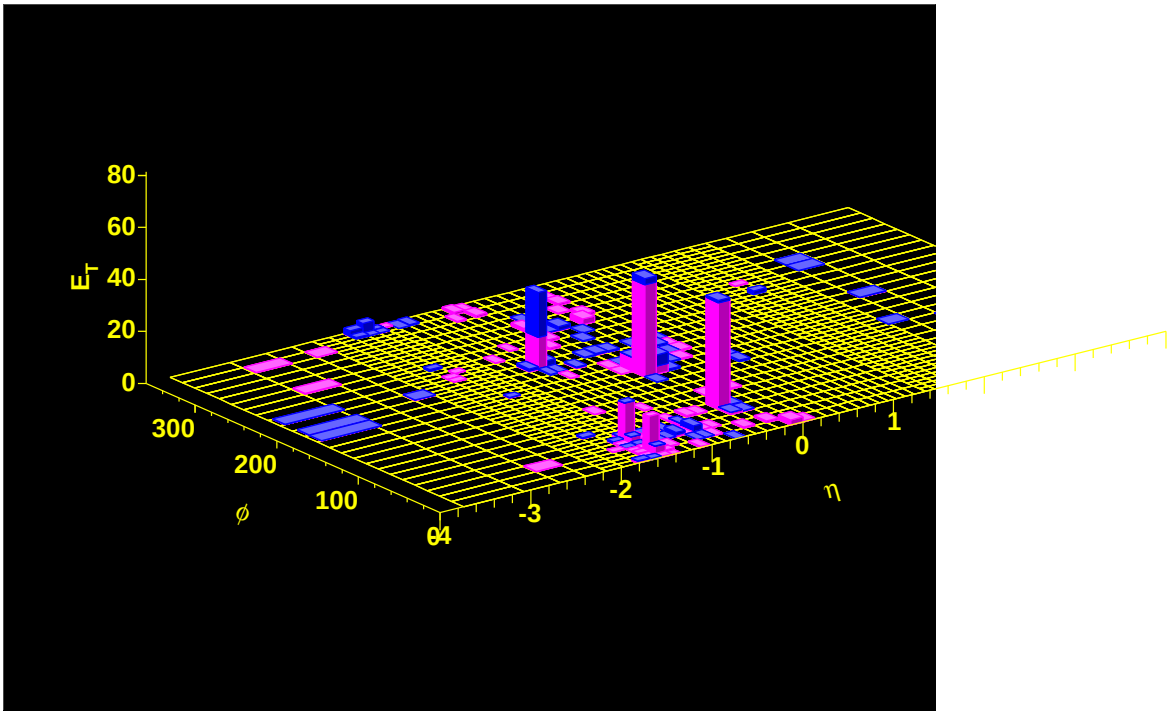

Figure 11: Calorimeter lego plot for run 167299, event 2376337 which is an eτ candidate.

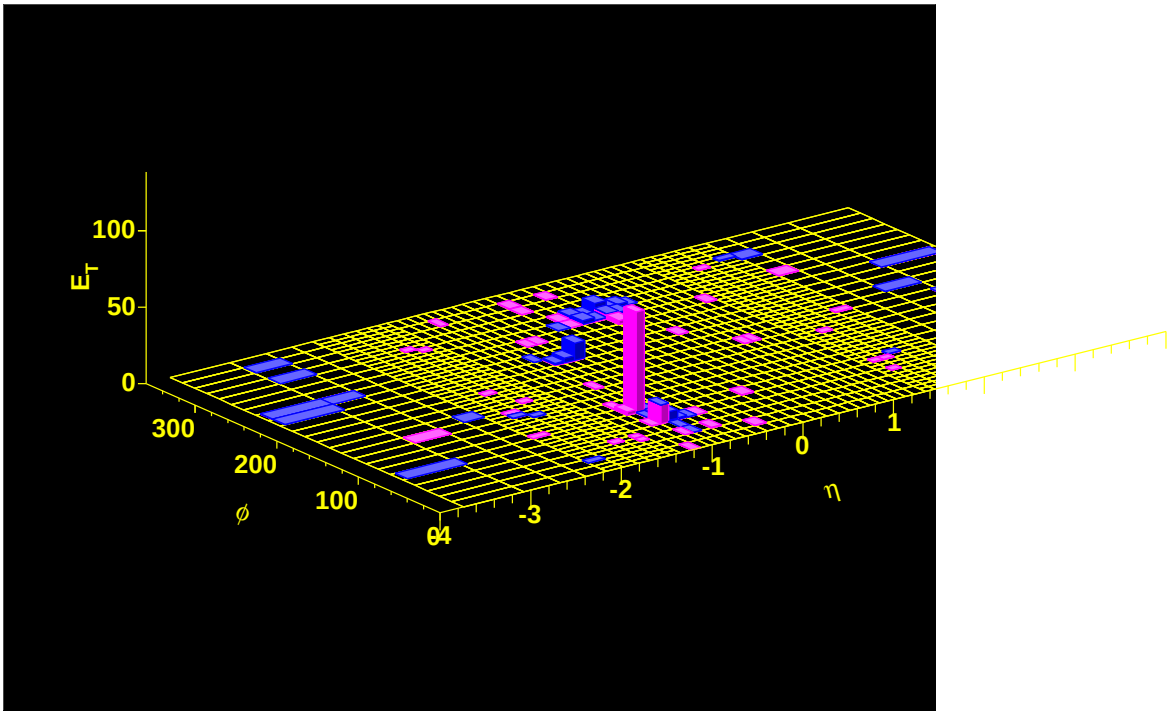

Figure 12: Calorimeter lego plot for run 151434, event 158200 which is an eτ candidate.

7 Result

This result provides no evidence for the the $e\tau$ or $\mu\tau$ plus jets final state in $t\bar{t}$-like events. Because of its relatively poor acceptance and high background, it is clear that the tau analysis can contribute little to a cross-section derived under the limit of lepton universality. Where this result can contribute, however, and what motivated this analysis in the first place, was the search for potentially anomalous contributions that could show up in the final state as an enhanced (or suppressed) rate for τ leptons in top decay.

To cast this analysis in this light, we choose to measure the parameter, r_τ where

$$r_\tau \equiv \frac{\mathrm{BR}(t \to b\tau\nu)}{\mathrm{BR}_{\mathrm{SM}}(t \to b\tau\nu)}.$$

One practical observable from which to derive r_τ is the ratio of measured rates for the $e\tau$+$\mu\tau$ dileptons to the ee, $e\mu$ and $\mu\mu$ dileptons. This observable ratio has several advantages experimentally, including largely common systematic uncertainties on acceptance. However, there is a problem with this technique in that a significant fraction (approximately 15% [24] under the assumption that $r_t au$ is unity) of the acceptance in the $\{e, \mu\}$ dilepton acceptance comes from tau leptons. Therefore, in the limit of very large r_τ, the ratio of the two rates becomes insensitive to r_τ, and, in fact, because the likelihood as a function of r_τ approaches a small but non-zero constant, the integral probability over a flat prior r_τ distribution is infinite.

Therefore, we choose instead to determine this variable by comparison to the standard model predicted rate. The probability distribution for the observable r_τ, given this measurement, is calculated by numerically integrating over hidden true variables representing the true $\sigma_{t\bar{t}}$ constrained by the uncertainties of the NNLO calculation [19], the standard model branching ratios, the number of $e\tau+\mu\tau$ dileptons predicted given $\sigma\times$BR, and the backgrounds to this analysis, all of which are constrained by experimental measurement or derivation.

The unnormalized probability distribution given this measurement as a function of r_τ is shown in Figure 13. The most probable value in this distribution is at $r_\tau \approx 0.8$.

This probability distribution can be used to set limits in the Bayesian approach by assuming a flat prior in r_τ. The resulting "one sigma" symmetric 68% confidence level range is

$$0.6 < r_\tau < 3.6 \text{ at } 68\% \text{ confidence.}$$

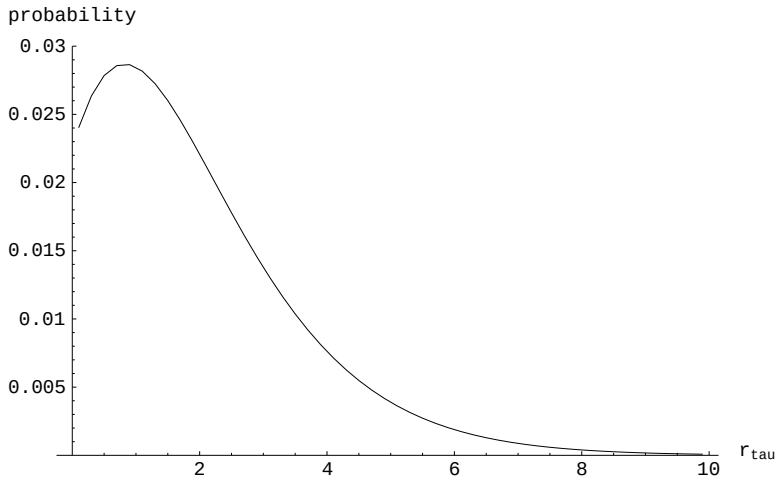

Figure 13: The unnormalized probability distribution $P(N_{\rm obs} = 2 \| r_\tau)$, where r_τ is the universality parameter

The 95% lower limit on r_τ is driven more by the requirement that $r_\tau > 0$ and the assumption of a flat prior than by the measurement as Figure 13 illustrates. We set therefore an upper limit,

$$r_\tau < 5.0 \text{ at } 95\% \text{ confidence},$$

which we consider the main result of this analysis. Clearly this measurement is consistent with the the lepton universality prediction of $r_\tau = 1$.

References

[1] J. Pumplin et al., "New Generation of Parton Distributions with Uncertainties from Global QCD Analysis", hep-ph/0201195 v3.

[2] M. Coca et al., "Winter 2003 Measurement of the t-tbar Cross Section in the Dilepton Decay Channel" CDF Note 6319

[3] Evelyn Thomson, "Description of data samples for Top and Electroweak groups for Winter 2003," CDF note 6742.

[4] `www-cdf.fnal.gov/internal/physics/ewk/hipt_lepton_baseline_cuts.h`

[5] M. Hohlmann, Ph.D. thesis, "Observation of Top Quark Pairs in the Dilepton Decay Channel Using Electrons, Muons, and Taus," CDF Note 4280

[6] S. Demers et al., "A Z Mass Cut to reduce $\gamma^*/Z \rightarrow \tau\tau$ background in the tau dilepton Analysis," CDF Note 6922

[7] K. McFarland et al., "Optimizing H_t and Jet E_t cuts in the $t\bar{t} \rightarrow \tau$ dilepton Analysis," CDF Note 6923

[8] M.Coca, E. Halkiadakis, "Central Electron Identification Efficiencies for Winter 2003 conferences," CDF Note 6262

[9] P. Murat, "W$\rightarrow \tau\nu$ Signal in Run II data and Preliminary measurement of BR(W$\rightarrow \tau\nu$)/BR(W$\rightarrow e\nu$)," CDF Note 6010

[10] S. Demers, et al., "Checking muon to tau fake with $Z \rightarrow \mu\mu$ data," CDF Note 6954.

[11] J. Conway, et al., "High pT Lepton ID Efficiency Scale Factor Studies," CDF Note 6858.

[12] W.K. Sakumoto, "W/Z Cross Section Predictions for sqrt(s)= 1.96 TeV," CDF Note 6341.

[13] A. Vaiciulis et al., "Estimating the Jet to Hadronic Tau Fake Rate," CDF Note 6784

[14] A. Hocker and W. Sakumoto, "Event $|z|<60$ cm Cut Acceptance for Run II", CDF Note 6917.

[15] Y-K Kim, et al., “Efficiencies for High P_T Electrons,” CDF Note 6234.

[16] K. Bloom, et al., “Muon Efficiencies”, CDF Note 6293.

[17] M. Coca et al., “Central Electron Identification Efficiencies”, CDF Note 6580.

[18] V. Martin and L. Cerrito, “Muon Cuts and Efficiencies for 4.11.1 Analyses”, CDF Note 6825.

[19] M. Cacciari et al., hep-ph/0303085. N. Kidonakis and R. Vogt, Phys. Rev. **D68** 114014 (2003).

[20] J. Insler et al., “Determining the Electron Fake Rate for Hadronic taus from the Data,” CDF Note 6408

[21] `http://www.physics.rutgers.edu/~zrwan/muon`

[22] M. Hohlmann, “Observation of Top Quark Pairs in the Dilepton Decay Channel Using Electrons, Muons, and Taus,” CDF Note 4280.

[23] S. Catani et al., “The top cross section in hadronic collisions”, Phys. Lett. B 378, 329 (1996).

[24] CDF Collaboration, “Measurement of the ttbar Cross-Section in Dilepton Events”, CDF Note 6882.